










SOURCE
DATATRANSPARENT
PROCESSOPEN
ACCESS

ciAPs control RIPK1 kinase activity-dependent and -independent cell death and tissue inflammation

Fabian Schorn^{1,†}, J Paul Werthenbach^{1,†} , Mattes Hoffmann¹, Mila Daoud¹ , Johanna Stachelscheid¹ , Lars M Schiffmann², Ximena Hildebrandt³ , Su Ir Lyu⁴ , Nieves Peltzer³, Alexander Quaas⁴, Domagoj Vucic⁵ , John Silke⁶ , Manolis Pasparakis^{7,8,9}  & Hamid Kashkar^{1,8,9,*} 

Abstract

Cellular inhibitor of apoptosis proteins (ciAPs) are RING-containing E3 ubiquitin ligases that ubiquitylate receptor-interacting protein kinase 1 (RIPK1) to regulate TNF signalling. Here, we established mice simultaneously expressing enzymatically inactive ciAP1/2 variants, bearing mutations in the RING domains of ciAP1/2 (ciAP1/2 mutant RING, ciAP1/2^{MutR}). *clap1/2*^{MutR/MutR} mice died during embryonic development due to RIPK1-mediated apoptosis. While expression of kinase-inactive RIPK1^{D138N} rescued embryonic development, *Ripk1*^{D138N/D138N}/*clap1/2*^{MutR/MutR} mice developed systemic inflammation and died postweaning. Cells expressing ciAP1/2^{MutR} and RIPK1^{D138N} were still susceptible to TNF-induced apoptosis and necroptosis, implying additional kinase-independent RIPK1 activities in regulating TNF signalling. Although further ablation of *Ripk3* did not lead to any phenotypic improvement, *Tnfr1* gene knock-out prevented early onset of systemic inflammation and premature mortality, indicating that ciAPs control TNFR1-mediated toxicity independent of RIPK1 and RIPK3. Beyond providing novel molecular insights into TNF-signalling, the mouse model established in this study can serve as a useful tool to further evaluate ongoing therapeutic protocols using inhibitors of TNF, ciAPs and RIPK1.

Keywords ciAP1; ciAP2; RIPK1; TNF; ubiquitin

Subject Categories Autophagy & Cell Death; Signal Transduction

DOI 10.15252/emboj.2023113614 | Received 27 January 2023 | Revised 28 August 2023 | Accepted 7 September 2023 | Published online 4 October 2023

The EMBO Journal (2023) 42: e113614

Introduction

Cellular inhibitor of apoptosis protein 1 and 2 (ciAP1 and ciAP2) are baculoviral inhibitor of apoptosis protein homologs encoded by the closely linked *Birc2* and *Birc3* genes and were first identified as components of the tumour necrosis factor receptor (TNFR) signalling complex (Rothe *et al*, 1995; Liston *et al*, 1996; Uren *et al*, 1996). The association of ciAPs with TNFR1 and TNFR2 requires interaction with TNF receptor-associated factor 2 (TRAF2; Rothe *et al*, 1995; Shu *et al*, 1996), which upon binding mediates TNF-induced gene expression via mitogen-activated protein kinases (MAPK) and nuclear factor κ B (NF κ B) signalling (Yeh *et al*, 1997). ciAP1 and ciAP2 exhibit high homology in their amino acid sequence and domain structures composed of three tandem amino-terminal baculovirus IAP repeats (BIRs) followed by a caspase recruitment domain (CARD) and a carboxy-terminal RING finger domain. Although the BIR domains direct the interaction with different factors such as TRAF2 (Samuel *et al*, 2006; Varfolomeev *et al*, 2006), the RING domain of ciAP1/2 catalyses ubiquitylation of target proteins, including autoubiquitylation, and controls increasingly complex and diverse cellular actions (Vaux & Silke, 2005). Accordingly, ciAPs ubiquitylate receptor-interacting protein kinase 1 (RIPK1), thereby blocking its kinase activity, and to inhibit TNF-mediated cell death, while promoting prosurvival signalling downstream of TNFR1 (Park *et al*, 2004; Bertrand *et al*, 2008; Mahoney *et al*, 2008; Varfolomeev *et al*, 2008; Moulin *et al*, 2012). In addition, ciAPs are known to promote the ubiquitylation and subsequent proteasomal degradation of NF κ B-inducing kinase (NIK) to block noncanonical

1 Faculty of Medicine and University Hospital of Cologne, Institute for Molecular Immunology, University of Cologne, Cologne, Germany

2 Faculty of Medicine and University Hospital of Cologne, Department of General, Visceral, Cancer and Transplantation Surgery, University of Cologne, Cologne, Germany

3 Faculty of Medicine and University Hospital of Cologne, Department of Translational Genomics, University of Cologne, Cologne, Germany

4 Faculty of Medicine and University Hospital of Cologne, Institute of Pathology and Center for Integrated Oncology (CIO) Cologne Bonn, University of Cologne, Cologne, Germany

5 Department of Immunology Discovery, Genentech, South San Francisco, CA, USA

6 The Walter and Eliza Hall Institute for Medical Research, Melbourne, Vic., Australia

7 Institute for Genetics, University of Cologne, Cologne, Germany

8 Faculty of Medicine and University Hospital of Cologne, Center for Molecular Medicine Cologne (CMMC), University of Cologne, Cologne, Germany

9 Cologne Excellence Cluster on Cellular Stress Responses in Aging-Associated Diseases (CECAD), University of Cologne, Cologne, Germany

*Corresponding author. Tel: +49 221 478 84091; E-mail: h.kashkar@uni-koeln.de

[†]These authors contributed equally to this work as first authors

NF κ B signalling in resting cells (Varfolomeev *et al.*, 2007; Vince *et al.*, 2007, 2009).

IAP antagonists that bind in the BIR2 and 3 grooves of cIAPs rapidly activate their E3 ubiquitin ligase activity leading to their autoubiquitylation. Ubiquitylated cIAPs then undergo rapid proteasomal degradation which, in turn, causes NIK accumulation on the one hand and RIPK1 kinase activity-dependent TNF-induced cell death on the other hand (Varfolomeev *et al.*, 2007; Vince *et al.*, 2007). Mice lacking either cIAP1 or cIAP2 are essentially normal (Conze *et al.*, 2005; Conte *et al.*, 2006) raising the possibility that cIAPs have redundant, or at least partially overlapping functions (Silke & Vaux, 2015). Loss of both cIAP1 and cIAP2 (*clap1*^{-/-}/*clap2*^{-/-}) causes lethality around embryonic day 10.5 (E10.5) indicating that cIAPs are required for embryonic development (Moulin *et al.*, 2012). Deletion of *Tnfr1* allowed *clap1*^{-/-}/*clap2*^{-/-} embryos to develop until birth and *clap1*^{-/-}/*clap2*^{-/-} embryos lacking either *Ripk1* or *Ripk3* survived until E12.5 or E15.5, respectively. These data suggest that cIAPs limit TNFR1-induced RIPK1/3-dependent cell death during embryonic development (Moulin *et al.*, 2012). A recent independent study showed that *clap1*^{-/-}/*clap2*^{-/-} embryos lacking *Caspase-8* and *Mkl1* only survived to birth suggesting that cIAPs also control cell death-independent processes in mouse embryos that can cause perinatal lethality (Zhang *et al.*, 2019a). Conditional deletion of *clap1/2* in adult mice caused inflammation and acute lethality, which was significantly alleviated, but not fully prevented with a combined deletion of *Caspase-8* and *Ripk3* (Zhang *et al.*, 2019a). While these studies show that control of TNF-induced cell death is a major physiological role of cIAPs, deficiency in cell death signalling could not completely rescue the knock-out phenotype. Thus, there is a still undefined role for cIAP1/2 in cell fate decisions.

Results

cIAP1/2 E3 ubiquitin ligase activity is required for embryonic development

In order to investigate the physiologic role of the E3 ubiquitin ligase activity of cIAPs, both *clap1/2* genes were targeted in parallel using CRISPR/Cas9 gene editing aiming to replace the critical phenylalanine by alanine at position 610 and 600 in cIAP1 and cIAP2, respectively (Mace *et al.*, 2008; Haas *et al.*, 2009; Feltham *et al.*, 2011). Sanger sequencing of the founder population revealed that none of the animals harboured the specific knock-in mutations; however,

one female was found to carry small deletions on both loci. For *clap1*, a 13 bp deletion was identified leading to a frameshift that shortens the protein by three amino acids introducing a premature stop codon at position 610 (T602LfsTer7; Fig EV1A). The *clap2* locus harboured an 8 bp deletion introducing a frameshift, which prolonged the mutant protein by 23 amino acids changing the phenylalanine at position 600 to a leucine (G601QfsTer34) (Fig EV1B). The founder female was backcrossed three times to C57BL/6N wild-type mice to eliminate possible CRISPR/Cas9-mediated off-target effects. Hereafter, the mutations introduced are termed cIAP1/2 mutant RING (cIAP1/2^{MutR}).

Intercrossing heterozygous *clap1*^{Wt/MutR}/*clap2*^{Wt/MutR} mice failed to produce progeny carrying homozygous cIAP1/2 RING mutations (*clap1*^{MutR/MutR}/*clap2*^{MutR/MutR}; Fig EV1C) indicating that these mice die during embryonic development. Further analyses showed that similar to *clap1*^{KO/KO}/*clap2*^{KO/KO} double knock-out (DKO) embryos, *clap1*^{MutR/MutR}/*clap2*^{MutR/MutR} embryos were present at the expected Mendelian frequencies (Fig EV1D) but showed signs of haemorrhage indicative of defects in vascular development between E10.5 and E11.5 (Fig 1A). Yolk sacs isolated from embryos at E10.5 exhibited reduced vascularisation while showing excessive caspase-3 cleavage (Fig 1B), suggesting that the E3 ubiquitin ligase activity of cIAP1/2 is required to prevent uncontrolled endothelial cell apoptosis during embryonic development. Our *in vitro* analyses using mouse embryonic fibroblasts (MEFs) showed that cIAP1 and cIAP2 MutR variants resisted birinapanant-induced degradation (Fig 1C). Furthermore, cIAP1/2^{MutR} MEFs accumulated NIK, providing confirmation that the cIAP1/2^{MutR} proteins lack E3 ubiquitin ligase activity (Fig 1C). In Wt MEFs, NIK could only be detected after birinapanant treatment. Furthermore, the expression levels of cIAP2^{MutR} and TRAF2 appeared lower in cIAP1/2^{MutR} MEFs, which may additionally contribute to NIK stabilisation as it requires a coordinated assembly of cIAP1/2 and TRAF2/3 protein complex (Zarnegar *et al.*, 2008; Dumetier *et al.*, 2020).

Consistent with previous reports (Haas *et al.*, 2009; Vince *et al.*, 2009; Annibaldi *et al.*, 2018), our analysis of the TNFR1 multi-protein complex using FLAG-tagged-TNF (FLAG-TNF) pull-down assay revealed the successful recruitment of TAB1, TRAF2, NEMO, the LUBAC component SHARPIN and RIPK1 to TNFR1 in Wt MEFs (Fig 1D). RIPK1 polyubiquitylation appeared 5 min after stimulation. In contrast, in cIAP1/2^{MutR} MEFs, neither TAB1, NEMO nor SHARPIN were detectably associated with the TNFR1 signalling complex. RIPK1 and TRAF2 were still present at the receptor complex; however, no polyubiquitylation pattern was observed. Instead,

Figure 1. cIAP1/2 E3 ubiquitin ligase activity is required for embryonic development.

- A Representative images of *clap1/2*^{Wt/Wt} (n = 5), *clap1/2*^{KO/KO} (n = 6), and *clap1/2*^{MutR/MutR} (n = 6) embryos isolated at E10.5. Arrowheads indicate haemorrhages.
- B Whole-mount yolk sacs isolated at E10.5 from *clap1/2*^{Wt/Wt} (n = 4), and *clap1/2*^{MutR/MutR} (n = 3) embryos, stained for CD31 (green) and cleaved caspase-3 (CC3) (red). White arrowheads indicate apoptotic endothelial cells. Scale bar: 100 μ m.
- C Western blotting (WB) of cIAP1/2^{Wt} and cIAP1/2^{MutR} MEFs. Cells were pretreated for 3 h with either DMSO or 20 μ M birinapanant (Biri.). Cell lysates were analysed for the expression of the indicated proteins (* indicates unspecific bands).
- D MEFs were treated with FLAG-TNF (1 μ g/ml) for the indicated times. TNFR1 protein complex was purified and analysed by WB.
- E MEFs were treated with TNF (100 ng/ml) for the indicated times. Cell lysates were analysed by WB.
- F IncuCyte analysis to determine % cell death in MEFs after treatment with increasing concentrations of TNF at indicated time points.
- G IncuCyte analysis to determine % cell death in MEFs after co-treatment with 5 μ M IDN-6556 (IDN) and increasing concentrations of TNF at indicated time points.

Data information: Data points in (F) and (G) represent mean \pm SEM of three technical replicates.
Source data are available online for this figure.

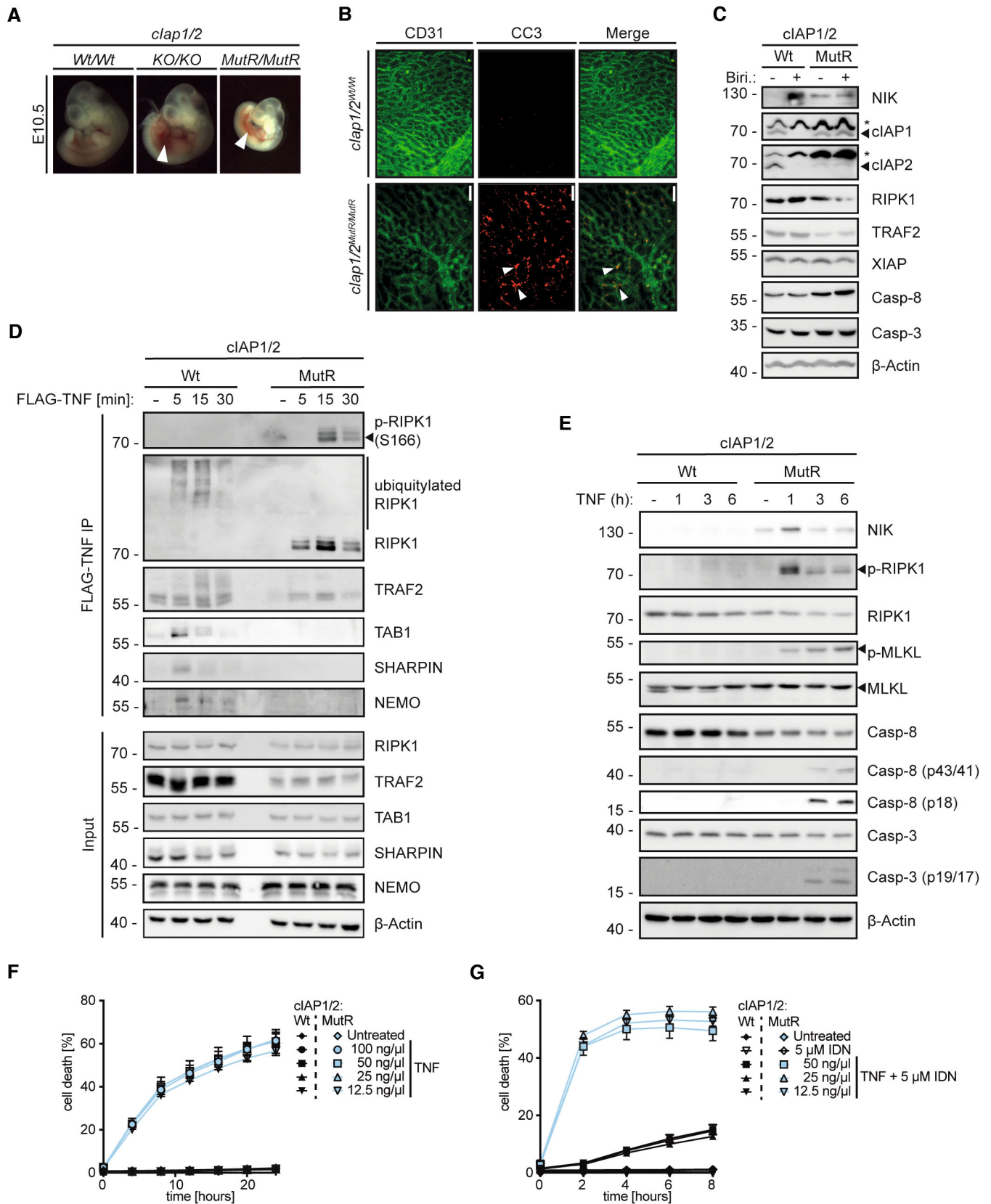


Figure 1.

in the $\text{cIAP1/2}^{\text{MutR}}$ MEFs, autophosphorylation of RIPK1 (S166) was detected 15 min after stimulation (Fig 1D) followed by caspase-8 and downstream caspase-3 cleavage at 3 h (Fig 1E). Additionally, MLKL phosphorylation was detected within 1 h of TNF stimulation, indicative of contemporaneous activation of necroptotic and apoptotic pathways in $\text{cIAP1/2}^{\text{MutR}}$ MEFs (Fig 1E). Delayed $\text{I}\kappa\text{B}\alpha$ phosphorylation/degradation, JNK and p38 MAPK signalling were detected in $\text{cIAP1/2}^{\text{MutR}}$ compared with Wt MEFs (Fig EV2A), implying that $\text{cIAP1/2}^{\text{MutR}}$ cells fail to adequately induce TNF-dependent NF κ B and MAPK signalling. Instead, lack of ubiquitylation leads to RIPK1 autophosphorylation and activation of necroptotic and apoptotic signalling. Accordingly, $\text{cIAP1/2}^{\text{MutR}}$ MEFs were highly susceptible to different concentrations of TNF (Fig 1F). Caspase inhibition by IDN-6556 (IDN) further facilitated TNF-induced cytotoxicity as a sign of ongoing necroptosis (Fig 1G). Additional studies using birinapant to deplete cIAPs in Wt MEFs revealed similar results considering the activation of caspase-8 and -3 (Fig EV2B). Phosphorylation of MLKL was, however, hardly detectable in Wt MEFs exposed to birinapant. Importantly, birinapant potentiated TNF-induced cell death in Wt MEFs (after 6 h); however, the susceptibility to TNF was markedly lower than $\text{cIAP1/2}^{\text{MutR}}$ MEFs (Fig EV2C). When caspase activity was blocked, birinapant-treated Wt MEFs were killed as efficiently as $\text{cIAP1/2}^{\text{MutR}}$ MEFs exposed to TNF. Birinapant could also increase TNF-induced cell death in $\text{cIAP1/2}^{\text{MutR}}$ MEFs, presumably due to its inhibitory activity towards XIAP. The RIPK1 inhibitor necrostatin-1S (Nec-1S) efficiently inhibited TNF-induced cell death (Fig EV2C), indicating that the loss of cIAP1/2 E3 ubiquitin ligase activity provokes susceptibility towards TNF-induced cell death controlled by RIPK1 kinase activity.

E3 ubiquitin ligase activity of cIAPs controls RIPK1 kinase activity-induced embryonic lethality

Based on our results obtained in cultured MEFs (Fig EV2C), RIPK1 kinase-inactive mice ($\text{Ripk1}^{\text{D138N/D138N}}$; Polykratis et al, 2014) were crossed into the $\text{clap1}^{\text{Wt/MutR}}/\text{clap2}^{\text{Wt/MutR}}$ background. $\text{Ripk1}^{\text{D138N/D138N}}/\text{clap1}^{\text{MutR/MutR}}/\text{clap2}^{\text{MutR/MutR}}$ mice survived embryonic development and were born at the expected Mendelian ratios (Fig EV1E). Yet, these mice had a significantly impaired median survival of only 35 days (Fig 2A). At birth, $\text{Ripk1}^{\text{D138N/D138N}}/\text{clap1}^{\text{MutR/MutR}}/\text{clap2}^{\text{MutR/MutR}}$ mice were indistinguishable from control animals ($\text{Ripk1}^{\text{D138N/D138N}}$ littermates); however, starting 7–10 days of postpartum, these mice appeared smaller. When

analysed at 12–25 days of age, these mice were runted, developed skin lesions (Fig 2B) and had a significantly reduced body weight compared with $\text{Ripk1}^{\text{D138N/D138N}}$ littermates (Fig 2C).

Livers from $\text{Ripk1}^{\text{D138N/D138N}}/\text{clap1}^{\text{MutR/MutR}}/\text{clap2}^{\text{MutR/MutR}}$ mice were significantly enlarged (Fig 2C) and histological examination (H&E) of liver sections revealed an inflammatory environment indicated by immune cell infiltrates (Fig 2D) and upregulated *Tnf* mRNA levels (Fig 2E). No excessive apoptosis or compensatory proliferation was detected in these livers. Remarkably, $\text{Ripk1}^{\text{D138N/D138N}}/\text{clap1}^{\text{MutR/MutR}}/\text{clap2}^{\text{MutR/MutR}}$ mice had a complete loss of liver resident Kupffer cells (Fig 2D). Similar to the livers, spleens from $\text{Ripk1}^{\text{D138N/D138N}}/\text{clap1}^{\text{MutR/MutR}}/\text{clap2}^{\text{MutR/MutR}}$ mice were enlarged (Fig 2C). Furthermore, spleen architecture was altered, and focal areas showed increased apoptosis (Fig EV2D). *Il6* and *Il1b*, but not *Tnf*, levels were strongly enhanced in spleens from $\text{Ripk1}^{\text{D138N/D138N}}/\text{clap1}^{\text{MutR/MutR}}/\text{clap2}^{\text{MutR/MutR}}$ animals (Fig 2E) indicating that the inflammatory conditions in the spleen were distinct from those in the liver. In contrast to liver and spleen, intestines isolated from $\text{Ripk1}^{\text{D138N/D138N}}/\text{clap1}^{\text{MutR/MutR}}/\text{clap2}^{\text{MutR/MutR}}$ mice at 12–25 days of age were histologically normal, and H&E sections revealed no obvious immune cell infiltration (Figs 2D and EV2D). However, mild increased expression of inflammatory cytokines including *Tnf*, *Il6* and *Il1b* was detected in the ileum (Fig 2E). Furthermore, *Tnf* expression was increased in the colon of $\text{Ripk1}^{\text{D138N/D138N}}/\text{clap1}^{\text{MutR/MutR}}/\text{clap2}^{\text{MutR/MutR}}$ mice compared with *Ripk1* mutant mice (Fig 2E). These data indicated that RIPK1 kinase activity is the main driver of the embryonic lethality in $\text{clap1}^{\text{MutR/MutR}}/\text{clap2}^{\text{MutR/MutR}}$ mice, whereas the postweaning multi-organ inflammation and the mortality of $\text{Ripk1}^{\text{D138N/D138N}}/\text{clap1}^{\text{MutR/MutR}}/\text{clap2}^{\text{MutR/MutR}}$ premature mice are mediated by RIPK1 kinase-independent processes.

TNF induces apoptosis and necroptosis in $\text{cIAP1/2}^{\text{MutR}}/\text{RIPK1}^{\text{D138N}}$ cells without involving RIPK1 kinase activity

Consistent with data using RIPK1 inhibitor Nec-1S in $\text{cIAP1/2}^{\text{MutR}}$ MEFs (Fig EV2C), expression of enzymatically inactive RIPK1^{D138N} efficiently blocked TNF-induced cell death in $\text{cIAP1/2}^{\text{MutR}}/\text{RIPK1}^{\text{D138N}}$ MEFs at early time points (up to 30 h post-treatment) (Figs 3A and EV3A). At late time points (beyond 30 h post-treatment), however, lack of RIPK1 kinase activity could not prevent TNF-induced cell death in either $\text{cIAP1/2}^{\text{MutR}}/\text{RIPK1}^{\text{D138N}}$ MEFs or $\text{cIAP1/2}^{\text{MutR}}$ MEFs cotreated with Nec-1S (Fig 3A). Western blotting

Figure 2. E3 ubiquitin ligase activity of cIAPs controls RIPK1 kinase activity-induced embryonic lethality.

- Kaplan–Meier survival curves of $\text{Ripk1}^{\text{D138N/D138N}}/\text{clap1/2}^{\text{Wt/Wt}}$ ($n = 7$) and $\text{Ripk1}^{\text{D138N/D138N}}/\text{clap1}^{\text{MutR/MutR}}/\text{clap2}^{\text{MutR/MutR}}$ ($n = 9$) mice. *P*-values were calculated with a log-rank (Mantel–Cox) test.
- Representative pictures of $\text{Ripk1}^{\text{D138N/D138N}}/\text{clap1/2}^{\text{Wt/Wt}}$ and $\text{Ripk1}^{\text{D138N/D138N}}/\text{clap1}^{\text{MutR/MutR}}/\text{clap2}^{\text{MutR/MutR}}$ mice at 2 weeks of age (white arrowhead indicates skin inflammation).
- Body weight, liver weight/body weight ratios (LW/BW), spleen weight/body weight ratios (SpW/BW) from age-matched mice of the indicated genotypes.
- Representative images of liver (upper panel) and ileum (lower panel) sections from mice at 2 weeks of age. Black arrowheads indicate apoptotic cells. Scale bars: 50 μm . Sections were stained with haematoxylin and eosin (H&E), cleaved caspase-3 (CC3), Ki67, or F4/80.
- Relative mRNA expression of the indicated genes from liver, spleen, colon, and ileum derived from $\text{Ripk1}^{\text{D138N/D138N}}/\text{clap1/2}^{\text{Wt/Wt}}$ ($n = 3$) and $\text{Ripk1}^{\text{D138N/D138N}}/\text{clap1}^{\text{MutR/MutR}}/\text{clap2}^{\text{MutR/MutR}}$ ($n = 4$) mice at 2 weeks of age measured by qPCR.

Data information: Dots in (C) represent individual mice and lines the mean. In (E), bars represent mean \pm SEM. *P*-values were calculated by one-way (C) or two-way (E) ANOVA with Bonferroni's postanalysis. **P* < 0.05; ***P* < 0.01; ****P* < 0.001; *****P* < 0.0001 and ns, not significant.

Source data are available online for this figure.

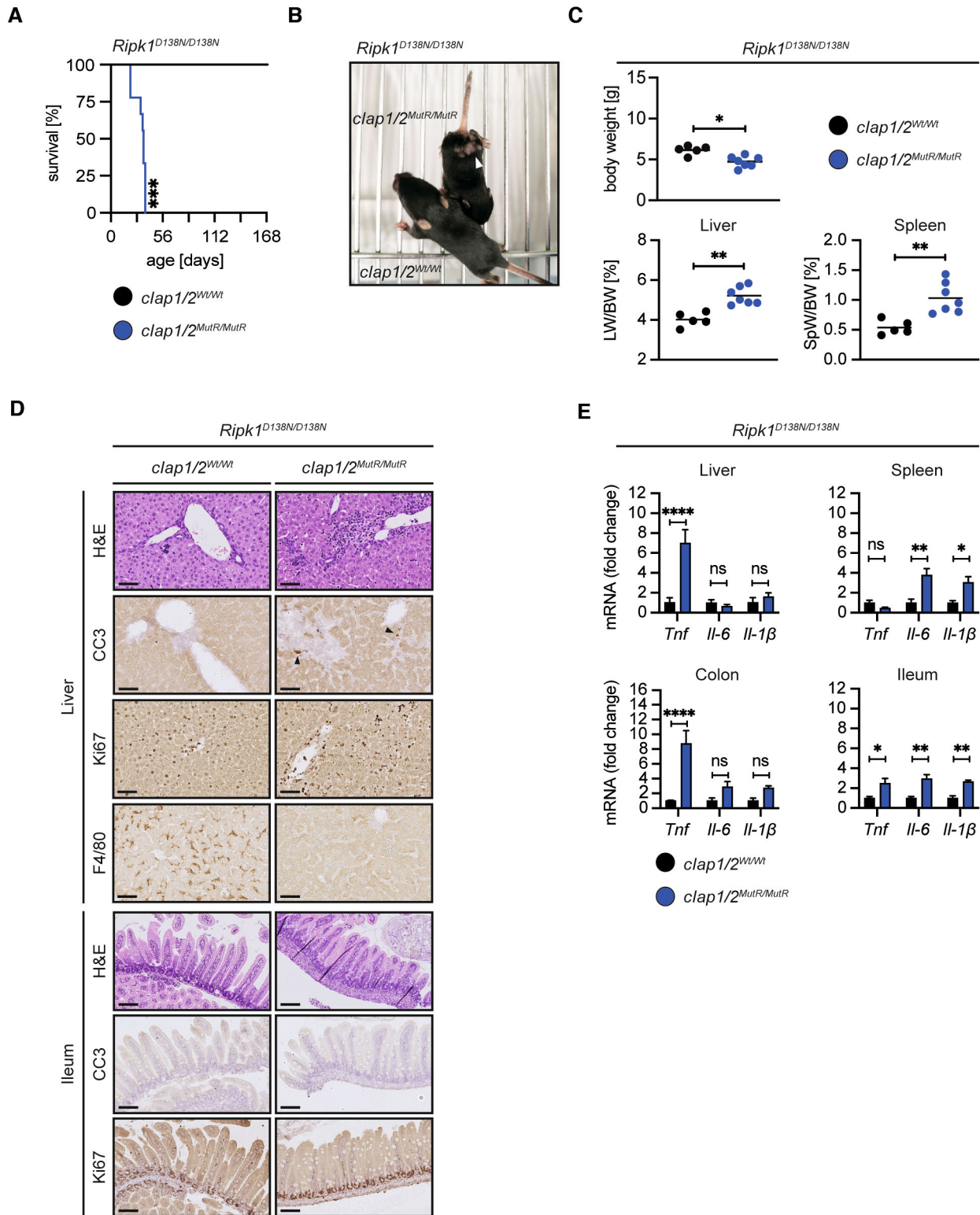


Figure 2.

(WB) showed that the lack of RIPK1 kinase activity efficiently reduced/delayed, but did not completely diminish, caspase activation in cells expressing cIAP1/2^{MutR} (Fig 3B).

If the residual caspase activity is responsible for TNF-induced late cell death of cIAP1/2^{MutR}/RIPK1^{D138N} MEFs, caspase inhibitor IDN should be able to diminish susceptibility of cells to TNF.

Surprisingly, when caspase activity was blocked, TNF exposure caused massive cell death (Figs 3C and EV3A and B) suggesting an increased necroptotic propensity of $\text{cIAP1/2}^{\text{MutR}}/\text{RIPK1}^{\text{D138N}}$ MEFs which was controlled by cIAPs but did not require RIPK1 kinase activity. WB analysis revealed a marked accumulation of phosphorylated RIPK3 in $\text{cIAP1/2}^{\text{MutR}}/\text{RIPK1}^{\text{D138N}}$ MEFs, which was further increased upon TNF (Fig 3B) or TNF/IDN (Fig 3D) treatment and followed by MLKL phosphorylation. These data collectively indicated that the lack of E3 ubiquitin ligase activity of cIAP1/2 potentiates apoptosis and, if caspase activity is inhibited, necroptosis in response to TNF which is not dependent on RIPK1 kinase activity. RIPK1 kinase-independent necroptosis (after TNF/IDN treatment) was efficiently blocked in $\text{cIAP1/2}^{\text{MutR}}/\text{RIPK1}^{\text{D138N}}$ MEFs when RIPK3 kinase activity was inhibited by GSK-872 (GSK) (Figs 3C and EV3A and B). Additional studies utilising specific knock-down of FADD in $\text{cIAP1/2}^{\text{MutR}}/\text{RIPK1}^{\text{D138N}}$ MEFs confirmed the data obtained by using IDN (Fig EV3C and D). FADD knock-down increased the susceptibility of $\text{cIAP1/2}^{\text{MutR}}/\text{RIPK1}^{\text{D138N}}$ to TNF (4-h treatment). Combined knock-down of FADD and RIPK3 in these cells efficiently diminished the susceptibility to TNF, further validating the data obtained by using IDN and GSK (Fig EV3C and D).

In agreement with our cell culture analyses, elevated phosphorylation of RIPK3 was also detected in the intestine and liver sections derived from $\text{Ripk1}^{\text{D138N/D138N}}/\text{clap1}^{\text{MutR/MutR}}/\text{clap2}^{\text{MutR/MutR}}$ mice (Fig 3E). In order to address the role of RIPK3 and necroptosis, we established $\text{Ripk3}^{\text{KO/KO}}/\text{Ripk1}^{\text{D138N/D138N}}/\text{clap1}^{\text{MutR/MutR}}/\text{clap2}^{\text{MutR/MutR}}$ mice. Lack of RIPK3 expression, however, did not ameliorate the observed phenotype. $\text{Ripk3}^{\text{KO/KO}}/\text{Ripk1}^{\text{D138N/D138N}}/\text{clap1}^{\text{MutR/MutR}}/\text{clap2}^{\text{MutR/MutR}}$ mice were runted and died prematurely resembling similar phenotypic alterations seen in $\text{Ripk1}^{\text{D138N/D138N}}/\text{clap1}^{\text{MutR/MutR}}/\text{clap2}^{\text{MutR/MutR}}$ mice (Fig 3F and G). These data indicated that necroptosis is not the driver of tissue inflammation and early lethality in $\text{Ripk1}^{\text{D138N/D138N}}/\text{clap1}^{\text{MutR/MutR}}/\text{clap2}^{\text{MutR/MutR}}$ mice. Notably, whereas the exposure to both GSK-872 and IDN could efficiently block TNF-induced cytotoxicity (Fig 3C and EV3A and B), GSK-872 treatment alone could not protect $\text{cIAP1/2}^{\text{MutR}}/\text{RIPK1}^{\text{D138N}}$ MEFs against TNF (Fig EV3B and E). These observations suggest that the increased susceptibility to TNF which is independent of RIPK1 kinase activity and RIPK3 may cause the lethal inflammatory phenotype in $\text{Ripk1}^{\text{D138N/D138N}}/\text{clap1}^{\text{MutR/MutR}}/\text{clap2}^{\text{MutR/MutR}}$ mice.

TNF binding to TNFR1 primarily triggers the formation of TNFR1-associated signalling complex called complex I, involving the adaptor protein TNFR1-associated death domain (TRADD; Hsu

et al, 1995) and RIPK1 (Silke, 2011). TRADD and RIPK1 interact with TRAF2 and FADD (Hsu et al, 1996) and direct cIAP1/2-mediated NF- κ B activation or caspase-8-mediated apoptosis, respectively. Previous genetic evidence demonstrated a pivotal interplay between TRADD and RIPK1 in controlling apoptosis (Ermolaeva et al, 2008; Anderton et al, 2019; Dowling et al, 2019). Our analysis of the TNFR1 multiprotein complex revealed the recruitment of TRAF2, NEMO, IKK2 and RIPK1 to TNFR1 in $\text{RIPK1}^{\text{D138N}}$ MEFs (Fig EV3F). RIPK1 polyubiquitylation appeared 5 min after stimulation. In contrast, in $\text{cIAP1/2}^{\text{MutR}}/\text{RIPK1}^{\text{D138N}}$ MEFs, neither NEMO nor IKK2 were detectably associated with the TNFR1 signalling complex, indicating the lack of TNF-induced NF κ B signalling. RIPK1 and TRAF2 were still present at the receptor complex; however, no polyubiquitylation pattern was observed. In $\text{cIAP1/2}^{\text{MutR}}/\text{RIPK1}^{\text{D138N}}$ MEFs, autophosphorylation of RIPK1 (S166) was not detectable (Fig EV3F). Thus, the lack of ubiquitin-mediated NF κ B/survival signalling and RIPK1-mediated cell death in $\text{cIAP1/2}^{\text{MutR}}/\text{RIPK1}^{\text{D138N}}$ MEFs may potentiate TRADD-dependent apoptosis. Indeed, specific knock-down of TRADD efficiently reduced TNF-induced cytotoxicity and caspase activity in $\text{cIAP1/2}^{\text{MutR}}/\text{RIPK1}^{\text{D138N}}$ MEFs (30-h treatment; Fig EV3G).

Combined loss of TNFR1 and RIPK1 kinase activity prolongs the lifespan of $\text{clap1}^{\text{MutR/MutR}}/\text{clap2}^{\text{MutR/MutR}}$ animals

To examine the role of TNFR1 in the lethality of $\text{cIAP1/2}^{\text{MutR}}/\text{RIPK1}^{\text{D138N}}$ mice, we first established $\text{Tnfr1}^{\text{KO/KO}}/\text{clap1}^{\text{MutR/MutR}}/\text{clap2}^{\text{MutR/MutR}}$ mice. Genetic ablation of the *Tnfr1* gene in $\text{clap1}^{\text{MutR/MutR}}/\text{clap2}^{\text{MutR/MutR}}$ mice restored the embryonic development (Fig EV1F) but only resulted in an extension of median survival to 25 days (Fig 4A) similar to $\text{Ripk1}^{\text{D138N/D138N}}/\text{clap1}^{\text{MutR/MutR}}/\text{clap2}^{\text{MutR/MutR}}$ mice (Fig 2A). $\text{Tnfr1}^{\text{KO/KO}}/\text{clap1}^{\text{MutR/MutR}}/\text{clap2}^{\text{MutR/MutR}}$ mice were runted, but in contrast to $\text{Ripk1}^{\text{D138N/D138N}}/\text{clap1}^{\text{MutR/MutR}}/\text{clap2}^{\text{MutR/MutR}}$ mice, did not show obvious signs of skin lesions, hepatomegaly or splenomegaly (Fig EV4A and B). Yet, $\text{Tnfr1}^{\text{KO/KO}}/\text{clap1}^{\text{MutR/MutR}}/\text{clap2}^{\text{MutR/MutR}}$ mice contained immune cell infiltrations surrounding the portal areas in the liver and a significant induction of *Tnf* and *Il1b* mRNA levels (Fig 4B–D). The appearance of liver macrophages (most likely Kupffer cells) in $\text{Tnfr1}^{\text{KO/KO}}/\text{clap1}^{\text{MutR/MutR}}/\text{clap2}^{\text{MutR/MutR}}$ mice is in contrast to the complete loss of liver macrophages in the $\text{Ripk1}^{\text{D138N/D138N}}/\text{clap1}^{\text{MutR/MutR}}/\text{clap2}^{\text{MutR/MutR}}$ mice (Fig 4D). Apoptotic areas in the spleen were still present in $\text{Tnfr1}^{\text{KO/KO}}/\text{clap1}^{\text{MutR/MutR}}/\text{clap2}^{\text{MutR/MutR}}$ animals

Figure 3. TNF induces apoptosis and necroptosis in $\text{cIAP1/2}^{\text{MutR}}/\text{RIPK1}^{\text{D138N}}$ cells without involving RIPK1 kinase activity.

- A IncuCyte analysis to determine % cell death in MEFs treated with TNF (100 ng/ml) and TNF + Nec-1S (20 μ M) at indicated time points.
 B MEFs were treated with TNF (100 ng/ml) and Nec-1S (20 μ M) for the indicated times. Cell lysates were analysed by WB.
 C IncuCyte analysis to determine % cell death of MEFs treated with TNF (100 ng/ml) and IDN-6556 (IDN) (5 μ M) and TNF, IDN and GSK-872 (GSK) (5 μ M), at indicated time points.
 D MEFs were treated with TNF/IDN for 4 h. Cell lysates were analysed by WB.
 E Representative images of liver and ileum sections from mice at 2 weeks of age. Black arrowheads indicate cells expressing phosphorylated RIPK3. Scale bars: 50 μ m.
 F Kaplan–Meier survival curves of $\text{Ripk3}^{\text{KO/KO}}/\text{Ripk1}^{\text{D138N/D138N}}/\text{clap1}^{\text{MutR/MutR}}/\text{clap2}^{\text{MutR/MutR}}$ ($n = 4$) and $\text{Ripk3}^{\text{KO/KO}}/\text{Ripk1}^{\text{D138N/D138N}}/\text{clap1}^{\text{MutR/MutR}}/\text{clap2}^{\text{MutR/MutR}}$ ($n = 5$) mice. *P*-values were calculated with a log-rank (Mantel–Cox) test.
 G Body weight, liver weight/body weight ratios (LW/BW), spleen weight/body weight ratios (SpW/BW) from age-matched mice of the indicated genotypes.

Data information: In (A) and (C), data is represented as mean of three technical replicates \pm SEM. *P*-values were calculated by repeated measures one-way ANOVA with Bonferroni's post analysis. Dots in (G) represent individual mice and lines the means. *P*-values calculated by unpaired Student's *t*-test. **P* < 0.05; ***P* < 0.01;

****P* < 0.001; *****P* < 0.0001 and ns, not significant.

Source data are available online for this figure.

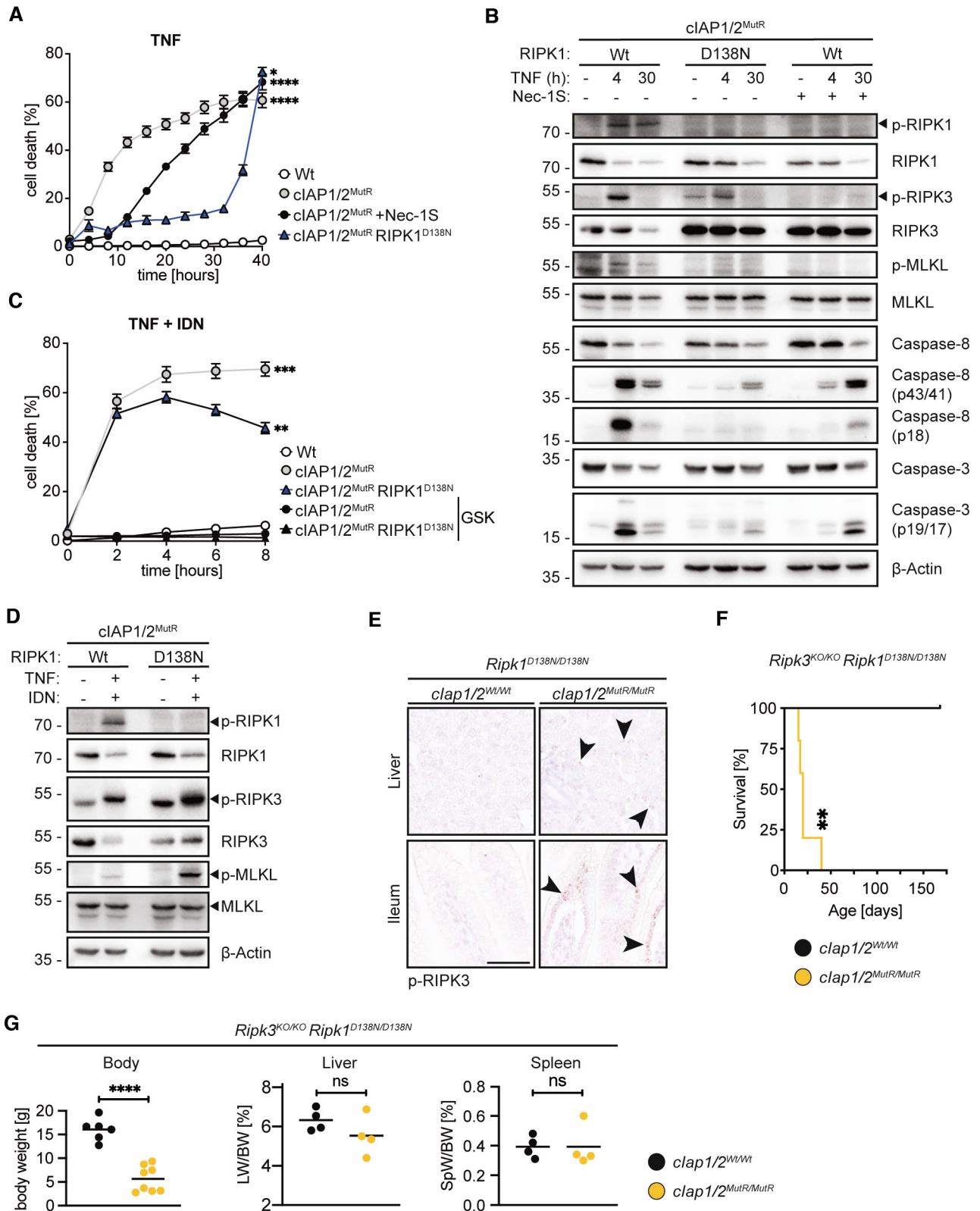


Figure 3.

(Fig EV4C); however, spleen cytokine levels were not altered compared with control littermates (Fig EV4D). Histological examination of the intestine revealed increased apoptosis in colon and ileum, which was not obvious in intestinal sections derived from *Ripk1^{D138N/D138N}/clap1^{MutR/MutR}/clap2^{MutR/MutR}* mice (Figs 4B and D, and EV4C).

Similar to *Ripk1^{D138N/D138N}/clap1^{MutR/MutR}/clap2^{MutR/MutR}* mice, additional ablation of *Ripk3* did not provide any phenotypical advantages in *Tnfr1^{KO/KO}/clap1^{MutR/MutR}/clap2^{MutR/MutR}* mice (Fig EV4E–G). Taken together, both *Ripk1^{D138N/D138N}/clap1^{MutR/MutR}/clap2^{MutR/MutR}* and *Tnfr1^{KO/KO}/clap1^{MutR/MutR}/clap2^{MutR/MutR}* mouse lines shared some phenotypic features and died prematurely by multi-organ inflammation without involving necroptosis. However, they differed in histology and inflammatory responses indicating that cIAPs control nonoverlapping signalling processes downstream of RIPK1 and TNFR1.

The role of RIPK1-independent TNF-induced cytotoxicity in *clap1^{MutR/MutR}/clap2^{MutR/MutR}* mice was investigated by combined ablation of TNFR1 expression and RIPK1 kinase activity. Consistent with the two individual mutant mouse lines, *Tnfr1^{KO/KO}/Ripk1^{D138N/D138N}/clap1^{MutR/MutR}/clap2^{MutR/MutR}* mice survived embryogenesis, were viable and born at the expected Mendelian ratios (Fig EV1G). Lack of both TNFR1 and RIPK1 kinase activity significantly increased the survival rate of *clap1^{MutR/MutR}/clap2^{MutR/MutR}* mice with a median survival of 100 days (Fig 4A). However, *Tnfr1^{KO/KO}/Ripk1^{D138N/D138N}/clap1^{MutR/MutR}/clap2^{MutR/MutR}* mice were still runted (Fig EV5A and B). Histological analysis in liver, spleen and intestinal sections derived from *Tnfr1^{KO/KO}/Ripk1^{D138N/D138N}/clap1^{MutR/MutR}/clap2^{MutR/MutR}* mice at 12–25 days of age showed no obvious alterations (Figs 4B and EV5C). The increased apoptosis seen in the intestinal sections of *Tnfr1^{KO/KO}/clap1^{MutR/MutR}/clap2^{MutR/MutR}* mice was absent upon inactivation of RIPK1 (Fig 4B and D). Likewise, the loss of macrophages in the livers of *Ripk1^{D138N/D138N}/clap1^{MutR/MutR}/clap2^{MutR/MutR}* mice (Fig 2D) was prevented by additional ablation of *Tnfr1* (Fig 4B and D). In line with these histological data, there was no pronounced upregulation of proinflammatory cytokines (Figs 4C and EV4D) collectively indicating that the early onset of the systemic inflammation and premature mortality are independently mediated by TNFR1 and RIPK1 kinase activity. Yet, *Tnfr1^{KO/KO}/Ripk1^{D138N/D138N}/clap1^{MutR/MutR}/clap2^{MutR/MutR}* mice were runty and had a short lifespan.

Although no signs of early systemic inflammation were observed, *Tnfr1^{KO/KO}/Ripk1^{D138N/D138N}/clap1^{MutR/MutR}/clap2^{MutR/MutR}* mice succumbed to a late-stage (beyond 100 days) inflammatory

phenotype observed predominantly in the liver and ileum (Fig 5A). Liver and ileal tissues taken from aged *Tnfr1^{KO/KO}/Ripk1^{D138N/D138N}/clap1^{MutR/MutR}/clap2^{MutR/MutR}* mice displayed signs of increased inflammation such as periportal immune infiltrates (Fig 5A). Massive immune cell infiltration was also detected in ileal sections of aged *Tnfr1^{KO/KO}/Ripk1^{D138N/D138N}/clap1^{MutR/MutR}/clap2^{MutR/MutR}* mice. In line with these findings, mRNA analysis showed an upregulation of *Tnf*, *Il1b* and *Ccl5* in liver and/or ileal tissues (Fig 5B). Histological investigation did not indicate any increased cell death in these tissues. Similarly, MEFs derived from *Tnfr1^{KO/KO}/Ripk1^{D138N/D138N}/clap1^{MutR/MutR}/clap2^{MutR/MutR}* mice were resistant to TNF-induced cell death (Fig EV5D).

NFκB-inducing kinase represents one important target of cIAP1/2 E3 ubiquitin ligase activity, which accumulated in cells expressing cIAP1/2^{MutR} (Fig 1C). Analysis of noncanonical NFκB activation revealed the processing of p100 (NFκB2) to p52 and accumulation of NIK in tissues derived from young and aged mice expressing cIAP1/2^{MutR} (Fig EV5E and F), which could not be completely blocked by ablation of TNFR1 and/or RIPK1 kinase activity. NIK inhibitor (Brightbill et al, 2018; Zhang et al, 2019a) diminished the expression of *Ccl4* and *Ccl5*, but not *Tnf*, in cIAP1/2^{MutR} MEFs (Fig EV5G) suggesting that NIK may partially contribute to the observed inflammatory phenotype. Its role in the hyperinflammatory phenotype observed in the aged *Tnfr1^{KO/KO}/Ripk1^{D138N/D138N}/clap1^{MutR/MutR}/clap2^{MutR/MutR}* mice remained unanswered.

Discussion

Previous studies exploring the physiologic role of cIAPs either by utilising chemical inhibitors of IAPs *in vivo* or by establishing gene knock-out mouse models indicated that cIAPs are important regulators of the TNF signalling machinery (Conze et al, 2005; Conte et al, 2006; Moulin et al, 2012; Zhang et al, 2019a). cIAP1 and cIAP2 act together with TRAFs and LUBAC to ubiquitylate RIPK1 and activate canonical p65/RelA NFκB in response to TNF. RIPK1 ubiquitylation is also required to block its autophosphorylation and subsequent activation of caspase-8-dependent apoptosis as well as RIPK3/MLKL-dependent necroptosis (Varfolomeev & Vucic, 2022). In general, genetic mouse models have shown that the ablation of *clap1/2* genes caused severe phenotypes and embryonic lethality that are, however, ameliorated only partially when major drivers of TNF-induced cytotoxicity such as caspase-8, RIPK3, MLKL or TNFR1 were genetically deleted in mice (Moulin et al, 2012; Zhang

Figure 4. Combined loss of TNFR1 and RIPK1 kinase activity prolongs the lifespan of *clap1^{MutR}/clap2^{MutR/MutR}* animals.

- A Kaplan–Meier survival curves of *Tnfr1^{KO/KO}/clap1/2^{Wt/Wt}* ($n = 7$), *Tnfr1^{KO/KO}/clap1/2^{MutR/MutR}* ($n = 11$), *Tnfr1^{KO/KO}/Ripk1^{D138N/D138N}/clap1/2^{Wt/Wt}* ($n = 10$) and *Tnfr1^{KO/KO}/Ripk1^{D138N/D138N}/clap1/2^{MutR/MutR}* ($n = 10$) mice. *P*-values were calculated with a log-rank (Mantel-Cox) test.
- B Representative images of liver and ileum sections from mice at 2 weeks of age. Scale bars: 50 μm. Sections were stained with Hematoxylin and Eosin (H&E), cleaved caspase-3 (CC3), Ki67, or F4/80. Arrowheads indicate CC3-positive staining.
- C Relative mRNA expression of the indicated genes from liver and ileum measured by qPCR. For ileal tissue samples 2 mice per genotype from *Tnfr1^{KO/KO}/clap1/2^{Wt/Wt}* and *Tnfr1^{KO/KO}/clap1/2^{MutR/MutR}* and 3 mice per genotype from *Tnfr1^{KO/KO}/Ripk1^{D138N/D138N}/clap1/2^{Wt/Wt}* and *Tnfr1^{KO/KO}/Ripk1^{D138N/D138N}/clap1/2^{MutR/MutR}* were measured.
- D Quantification of cells positive for cleaved caspase-3 (CC3), Ki67, or F4/80 staining in liver and ileum sections of mice.

Data information: In (C), bars represent mean ± SEM of three mice per genotype for liver samples. *P*-values were calculated using two-way ANOVA followed by Bonferroni postanalysis and significance is visualised in comparison with *Tnfr1^{KO/KO}* controls. In (D), each data point represents one mouse and bars indicate mean ± SD.

****P* < 0.001.

Source data are available online for this figure.

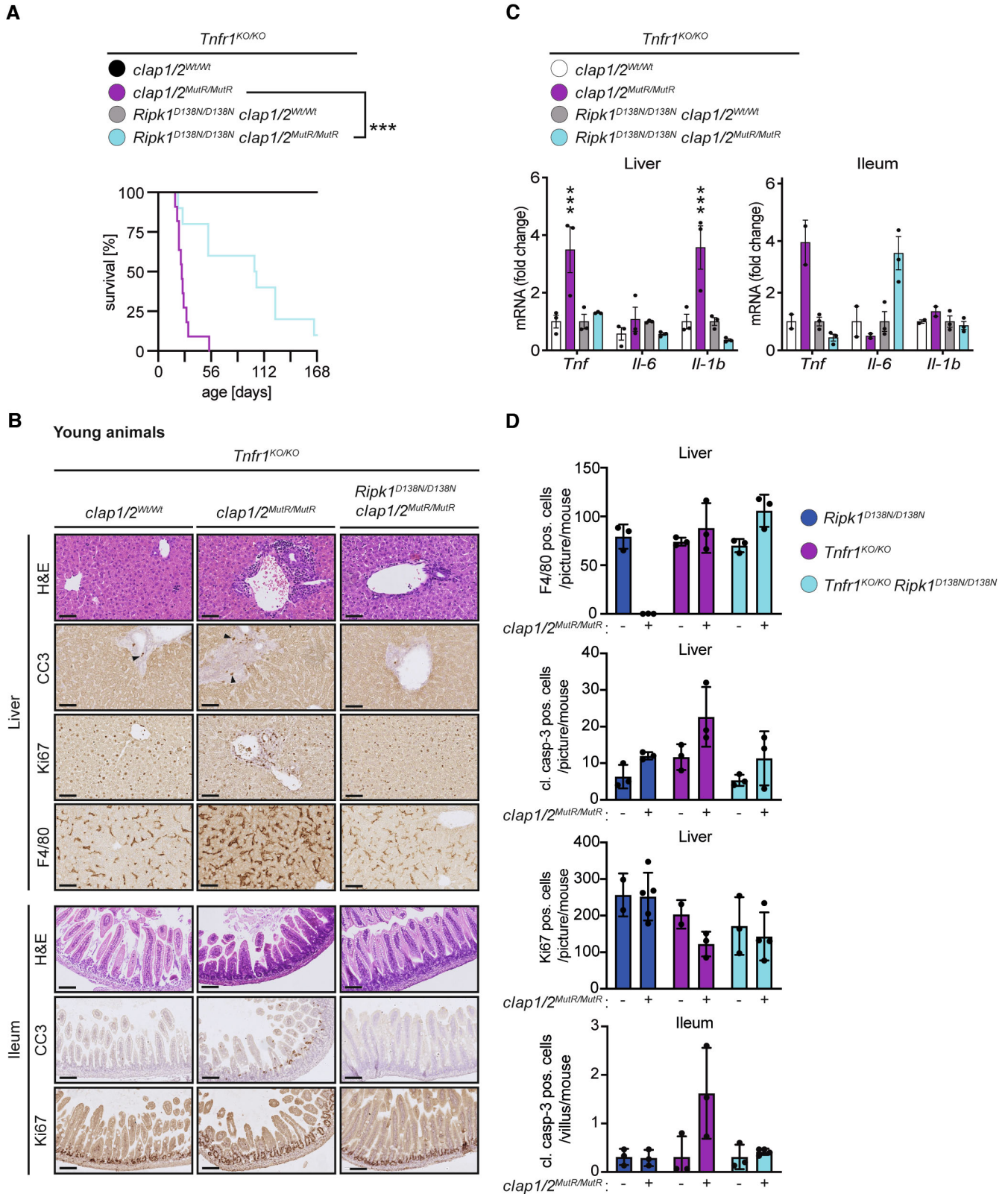


Figure 4.

et al, 2019a). By establishing *clap1^{MutR/MutR}/clap2^{MutR/MutR}* mice specifically lacking cIAP1/2 functional RING domains, we could show that the lack of E3 ubiquitin ligase activity of cIAPs causes embryonic lethality. This embryonic lethality could be rescued to post-weaning by solely inactivating RIPK1 kinase activity, and therefore indicate that RIPK1 and particularly its kinase activity is an

important target of cIAP1/2's E3 ligase activity. This extends earlier work showing that *Ripk1* gene ablation prolonged the embryonic survival of *clap1^{-/-}/clap2^{-/-}* mice from E10 to E12.5 (Moulin et al, 2012). It is important to note that our studies involving cell death assays, and protein expression/interaction, ubiquitylation, and phosphorylation conclusively validated the lack of E3 ubiquitin

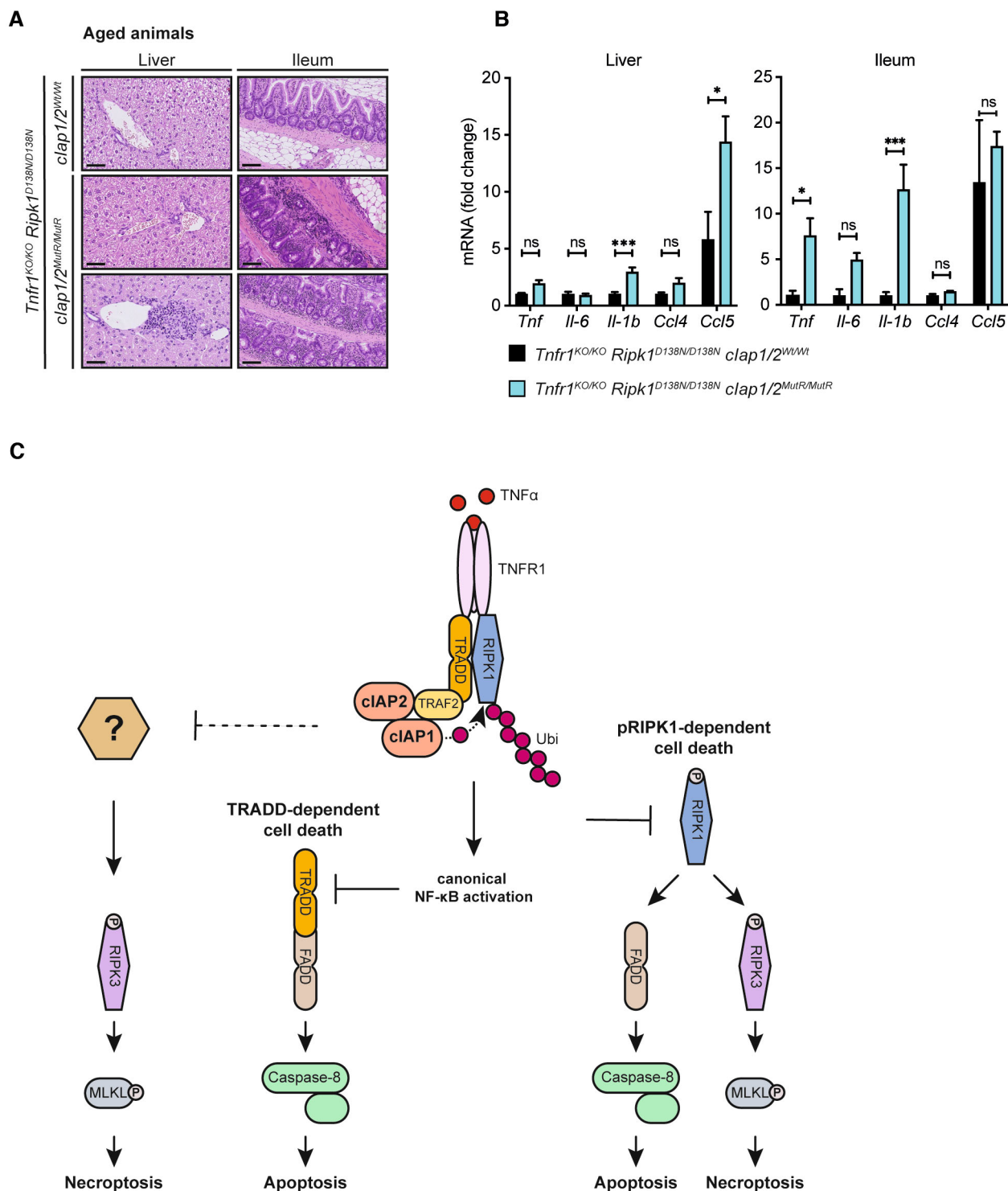


Figure 5.

Figure 5. Hyperinflammatory phenotype in the aged *Tnfr1^{KO/KO}/Ripk1^{D138N/D138N}/clap1/2^{MutR/MutR}* mice.

- A Representative images of liver and ileum sections from mice with the indicated genotypes at 24 weeks of age. Scale bars: 50 μ m (liver) and 100 μ m (ileum).
- B Relative mRNA expression of the indicated genes from liver and ileum isolated from mice measured by qPCR. Bars represent mean of three mice per genotype \pm SEM. *P*-values were calculated using two-way ANOVA followed by Bonferroni postanalysis. **P* < 0.05; ****P* < 0.001 and ns, not significant.
- C Schematic illustration of cIAP-mediated control of TNFR1-induced cell death. The ubiquitin ligase activity of cIAP1/2 controls TNF-induced RIPK1-mediated apoptosis/necroptosis and provides the molecular platform for the activation of NF κ B in response to TNF. Activation of NF κ B survival signalling inhibits TNF-induced TRADD-mediated apoptosis. cIAP-mediated ubiquitylation further controls TNF-induced RIPK3-dependent and RIPK1-independent necroptosis. The underlying molecular mechanism remains undetermined.

Source data are available online for this figure.

ligase activity of cIAP1/2^{MutR}. These data, however, cannot formally exclude that the introduced mutations in the RING domain of cIAP1/2 may have additional impact on protein function beyond its E3 ubiquitin ligase activity.

RIPK1 kinase activity and its autophosphorylation are crucial for the formation of RIPK1-containing protein complexes inducing either caspase-8-mediated apoptosis or RIPK3-mediated necroptosis, which have been considered as the major targets of cIAPs (Varfolomeev & Vucic, 2022). Our data, however, showed that in cIAP1/2^{MutR}/RIPK1^{D138N} cells, RIPK1 kinase activity is not required for TNF-induced apoptosis and necroptosis. On the contrary, the marked necroptotic propensity of cIAP1/2^{MutR}/RIPK1^{D138N} cells was reliant on RIPK3 kinase activity and was associated with elevated levels of phosphorylated RIPK3 in cultured cells and mouse tissues. Nevertheless, the inflammatory tissue damage seen in both *Ripk1^{D138N/D138N}/clap1^{MutR/MutR}/clap2^{MutR/MutR}* and *Tnfr1^{KO/KO}/clap1^{MutR/MutR}/clap2^{MutR/MutR}* mice could not be ameliorated by ablation of the *Ripk3* gene, demonstrating that necroptosis is extremely unlikely to contribute to the observed inflammatory phenotype. Notably, recent studies have shown that mutating the ubiquitylation site K376 of RIPK1 (K376R) causes embryonic lethality (Tang et al, 2019; Zhang et al, 2019b; Kist et al, 2021), closely resembling the phenotypic alterations observed in our *clap1^{MutR/MutR}/clap2^{MutR/MutR}* mice. The observed embryonic lethality was effectively prevented by treatment of RIPK1 kinase inhibitor and was rescued by deletion of the *Tnfr1* gene. Similar to the *Tnfr1^{KO/KO}/clap1^{MutR/MutR}/clap2^{MutR/MutR}* mice in our studies, *Tnfr1^{KO/KO}/Ripk1^{K376R/K376R}* mice displayed systemic inflammation and died within 2 weeks (Tang et al, 2019; Zhang et al, 2019b; Kist et al, 2021), together underscoring cIAP1/2 as the key regulatory E3 ubiquitin ligases targeting K376 of RIPK1. In contrast to *Tnfr1^{KO/KO}/clap1^{MutR/MutR}/clap2^{MutR/MutR}* mice in our study, however, additional deletion of *Ripk3* could block inflammatory tissue damage and lethality of *Tnfr1^{KO/KO}/Ripk1^{K376R/K376R}* mice (Zhang et al, 2019b). Our observations clearly indicated that cIAP1/2 not only control TNFR1-mediated RIPK1-dependent cytotoxicity and, thus, the lack of cIAP1/2 E3 ubiquitin ligase activity engages RIPK1-dependent and -independent cell death/inflammatory processes ultimately leading to tissue damage (Fig 5C). These observations are consistent with previous studies using various cellular settings and showing that TNF-induced apoptotic and necroptotic cell death pathways can be RIPK1 independent (Wong et al, 2010; Vanlangenakker et al, 2011; Moujalled et al, 2013). TRADD is a key adaptor protein for TNFR1, which can induce both NF κ B and apoptosis in response to TNF (Hsu et al, 1995, 1996). Inhibition of NF κ B potentiates TRADD-mediated apoptosis (Micheau & Tschopp, 2003). Furthermore, previous genetic evidence suggested that RIPK1 limits TRADD-induced apoptosis (Anderton et al, 2019). Thus, the lack of RIPK1 kinase activity

and NF κ B activation together can provoke TNF-induced apoptosis by involving TRADD. Accordingly, the transient knock-down of TRADD in cIAP1/2^{MutR}/RIPK1^{D138N} cells reduced TNF-induced cell death (Fig EV3G). However, physiologic relevance of these findings and the role of TRADD in the inflammatory phenotype seen in *Ripk1^{D138N/D138N}/clap1^{MutR/MutR}/clap2^{MutR/MutR}* mice remained unanswered.

The fact that cells or tissues derived from *Tnfr1^{KO/KO}/Ripk1^{D138N/D138N}/clap1^{MutR/MutR}/clap2^{MutR/MutR}* mice did not show any signs of cell death raises the possibility that the aberrant activation of the noncanonical NF κ B pathway may cause systemic inflammation and mortality. This is in line with previous studies characterising *clap2^{H570A/H570A}* mice (Conze et al, 2010). Site-directed mutagenesis of the Zn²⁺-coordinating histidine residue in the RING domain of cIAP1 (H582A) or cIAP2 (H570A) do not lead to severe phenotypic alteration in mice and both *clap1^{H582A/H582A}* and *clap2^{H570A/H570A}* mice are viable and fertile (Conze et al, 2010; Giardino Torchia et al, 2013). *clap2^{H570A/H570A}* mice, however, accumulated abnormal B cells with gut-associated lymphoid hyperplasia (after 6–7 months of age) as a consequence of an elevated noncanonical NF κ B signalling, indicating that cIAP2 E3 ubiquitin ligase activity is required to block NIK in lymphoid organs (Conze et al, 2010). Furthermore, keratinocyte-specific loss of TRAF2 causes psoriasis-like skin inflammation which can be prevented only by combined ablation of TNF and noncanonical NF κ B signalling (Etemadi et al, 2015), further underscoring the eminent role of noncanonical NF κ B activation in inflammatory phenotypes induced by alteration of TRAF2 and cIAPs. Interrogating the adverse effects of the noncanonical pathway on *Tnfr1^{KO/KO}/Ripk1^{D138N/D138N}/clap1^{MutR/MutR}/clap2^{MutR/MutR}* mouse survival requires additional genetic approaches.

The mouse model established in this study represents a suitable model to further investigate the important regulatory functions of cIAP1/2 and can provide new insights in TNF signalling and its impact on human diseases. Given the therapeutic value of cIAPs and RIPK1 in multiple clinical trials (Kashkar, 2010; Morrish et al, 2020; Newton, 2020), mechanistic understanding of how E3 ubiquitin ligases cIAP1/2 control RIPK1 and other signalling moieties may help to identify specific human diseases that would benefit from such targeting strategies.

Materials and Methods

Experimental model and subject details

Mice

TNFR1^{KO/KO} (Van Hauwermeiren et al, 2013), *Ripk1^{D138N/D138N}* (Polykratis et al, 2014) and *Ripk3^{KO/KO}* (Newton et al, 2016) mice

were described in previous studies. Homozygous *cIAP1*^{KO/KO} *cIAP2*^{KO/KO} mice have been described previously (Moulin *et al*, 2012). All mice were housed at the CECAD animal facility (University of Cologne, Germany) under SPF (standard pathogen-free) conditions with a 12-h light/dark cycle. Water and food were provided *ad libitum*. Mouse studies were performed after approval by the local authorities (LANUV, NRW, Germany) and in accordance with the German animal protection laws (Ref. number: AZ84.02.04.2015.A471, AZ84.02.04.2019.A145, AZ84.02.04.2021.A123). Study-specific calculations regarding group size, randomisation and study blinding were not performed. Mice were grouped according to their genotypes in groups of mixed sexes.

Generation of *clap1/2*^{MutR/MutR} mice

clap1^{MutR/MutR}/*clap2*^{MutR/MutR} mice were generated by simultaneous pronuclear injections (PNI) of C57BL/6N zygotes (Fritsch *et al*, 2019) with two single-guide RNAs (sgRNAs) targeting *Birc2* (*clap1*) and *Birc3* (*clap2*). Gene-specific sgRNAs (*Birc2*: 5'-TCTGCAGGGGACAATCAAG-3'; *Birc3*: 5'-ATCTGTAGAGGGAC-CATCA-3') were generated via *in vitro* transcription (IVT). An injection solution was prepared containing both sgRNAs (each at 10 ng/μl), two single template DNA strands (*Birc2*: 5'-CCCTTCTC TAAGGAAGTCCCCATCTGCAGGGGACAATTAAGGAAGTGTGC GCACAGCGTCTCATGAGTGAAGAATGGTCTGAAAGTATTGTTGG ACATCAGAAGCTGTGACAACA-3'; *Birc3*: 5'-TCCCTCTCTGAGGAAG TGTCCCATCTGTAGA G GGACCATTAAGGCACAGTGGCACAGC GCTCTCTGAACAAGACTAATGGTCCATGGCTGCAACTTCAGCCAG GAGGAAGTTCCTG-3') (25 ng/μl), and 30 ng/μl Cas9 mRNA (TriLink Biotechnologies). Pronuclear injections (PNI) were performed at the CECAD *in vivo* Research Facility (University of Cologne, Germany). One founder animal, carrying short deletions in both genes, was backcrossed for three generations into the C57BL/6N background to eliminate possible off-target effects.

MEF cell culture

Mouse embryonic fibroblasts (MEFs) were generated from embryos of indicated genotypes harvested at E10.5 (Andree *et al*, 2014) and cultured in Dulbecco's Modified Eagle Medium (DMEM) (Bio&Sell) supplemented with 10% heat-inactivated fetal bovine serum (Biowest), 2 mM L-glutamine (Biochrom), 10 mM HEPES (pH 7.2) (Fisher BioReagents), 1× nonessential amino acids (Merck), 100 U ml⁻¹ penicillin and 100 μg ml⁻¹ streptomycin (Bio&Sell). Mouse embryonic fibroblasts were immortalised using simian virus 40 (SV40) transformation. Afterwards, cells were expanded for several passages before being used in following experiments.

Method details

Embryology and immunofluorescence

For timed breeding, *clap1*^{Wt/MutR}/*clap2*^{wt/MutR} heterozygous animals were paired. Females were screened daily for vaginal plugs and a positive plug determined embryonic day (E) 0.5. Further, a gain in weight by > 2 g after 10 days was used as an additional marker for a potential pregnancy. Embryos were isolated at E10.5. Pictures were taken using a M80 stereomicroscope (Leica) equipped with a IC80 HD microscope camera (Leica). Yolk sacs were collected, washed in phosphate-buffered saline (PBS) and fixed with 3% PFA (paraformaldehyde). Afterwards, yolk sacs

were incubated with anti-cleaved Caspase-3 (Rabbit; #9661; Cell Signaling) and anti-CD31 (Armenian hamster; #ab119341; abcam) (overnight) before adding the secondary antibodies, anti-Rabbit IgG Alexa Fluor 594 (Goat; #A11012; Life Technologies) and anti-Armenian hamster IgG FITC (Goat; #ab5739; abcam) for 1 h at room temperature (Schiffmann *et al*, 2020). Pictures were taken using a motorised inverted Olympus IX81 microscope (Cell^R Imaging Software). Adobe Photoshop (version 22.1.0) was used for editing.

Immunoprecipitation (IP)

Cells were exposed to 1 μg/ml recombinant FLAG tagged mouse TNF-α (#ALX-522-009; Enzo), rinsed with ice-cold PBS and placed on ice to stop the stimulation. PBS was removed and 150 μl DISC lysis buffer (30 mM Tris-HCl, pH 7.5, 150 mM NaCl, 10% glycerol, 1% Triton X-100, 2 mM EDTA, supplemented with 1× PhosSTOP (Roche), 1× cOmpleteTM protease inhibitor (Roche) and 0.5 mg/ml NEM (Sigma-Aldrich)) was added directly onto the plates. Cells were scraped off, collected in 1.5-ml tubes and placed on ice for 20 min. The cell suspension was centrifuged for 20 min at 20,000 g at 4°C to remove cell debris. The cleared lysates were transferred to fresh 1.5-ml tubes. A fraction of each sample was collected separately and served as input control. The remaining lysate fractions were processed according to the manufacturer's protocol using the μMACSTM DYKDDDDK Isolation Kit (Miltenyi Biotec) (washing with the Wash Buffer 1 was reduced to 1 × 200 μl). All antibodies used are summarised in Appendix Table S1.

Cell death measurements

Cells (0.75 or 1 × 10⁴) were seeded onto 96-well plates coated with 1% gelatin in MEF culture medium. The next day, cells were washed once with PBS before adding 100 μl medium containing indicated stimuli and 0.15 μM DRAQ7TM (biostatus). Cells were pretreated with DMSO (Carl Roth) as control treatment or 20 μM Birinapant (Biozol) 3 h prior and throughout stimulation to induce efficient cIAP1/2 depletion. In siRNA knock-down experiments, 10⁴ cells were seeded on 96-well plates and transfected with the respective siRNA for 24 h using Lipofectamine[®] RNAi MAXTM (Invitrogen) according to the manufacturer's instructions (Daoud *et al*, 2022), before adding TNF and 0.15 μM DRAQ7TM (biostatus) or 1 μM cellEventTM Caspase-3/7 (Invitrogen). The following siRNAs were used: siTRADD (5'-GGUUCGAAGUUCGCGUUU-3'), siRIPK3 (5'-AAGAUUAACCAUAGCCUUCACCUCCA-3') (Kearney *et al*, 2014). siRNAs were designed and/or purchased from Eurofins Genomics. siFADD was from ThermoFisher #AM16704. Prepared 96-well plates were placed into the IncuCyte[®] Live-Cell Analysis System (Sartorius), where cell death was measured for up to 48 h. Percent cell death was calculated mainly by normalisation to the number of seeded cells or number of total cells at the final time point, measured through lysis of each well with 200 μg/ml digitonin (Sigma Aldrich).

Quantitative real-time PCR (qPCR)

qPCR analysis was performed on cDNA generated from MEFs or frozen tissues samples, using gene specific primers and the Light-Cycler[®] 480 SYBR[®] Green I Mix (Roche). qPCRs were run on the CFX96TM Real-Time System (Bio-Rad). *Actb* was used as

housekeeping gene and data were further analysed as previously described using the LingRegPCR program (Ramakers *et al*, 2003).

Immunohistochemistry (IHC)

Liver, spleen and intestinal tissue were fixed in ROTI® Histofix 4% (Carl Roth), embedded in paraffin and cut in 5 µm sections. After deparaffinisation and endogenous peroxidase blocking (40 mM sodium citrate, 12.1 mM Na₂HPO₄, 30 mM NaN₃, 3% H₂O₂) for 15 min at room temperature, samples were further treated by either heat-induced antigen retrieval (10 mM sodium citrate, 0.05% Tween-20, pH 6.0), or proteinase K digest (Qiagen) (in 50 mM Tris, pH 8.0, 1 mM EDTA, 0.5% Triton-100). In between two washing steps with PBS + 0.05% Tween-20, sections were blocked for 1 h at room temperature in a wet chamber using the Avidin/Biotin Blocking Kit (Vector Laboratories). Samples were incubated over night at 4°C in the appropriate primary antibodies (Appendix Table S1). The next day, sections were incubated with the corresponding biotinylated secondary antibodies (Appendix Table S2). Finally, the ABC HRP Kit Vectastain Elite (Vector Laboratories) and the DAB staining Kit (Dako) were used for visualisation and counterstained with Hematoxylin (Carl Roth) (Fritsch *et al*, 2019).

Stained sections were scanned with an SCN4000 Slide Scanner (Leica) and an NanoZoomer S360 Digital slide scanner (Hamamatsu) and analysed with the imaging software Aperio ImageScope v.12.2.2.5015 (Leica). Pictures present in this work are representative for at least three mice per genotype. For quantification of liver sections, F4/80, cleaved caspase-3, and Ki67-positive cells were counted in frames of identical size (16.3 × 10.2 cm; F4/80: mean of four frames at 40× magnification, cleaved caspase-3: one frame at 10× magnification, Ki67: one frame at 20× magnification). Cleaved caspase-3 positive cells in the ileum were quantified as previously described (Fritsch *et al*, 2019). 15 villi per mouse were analysed for the quantification.

Quantification and statistical analysis

Microsoft® Excel for Mac (version 16.52; Microsoft) and GraphPad Prism for macOS (version 8.4.3; GraphPad Software, LLC.) were used for statistical analysis. Data are displayed as mean ± SEM. * indicates $P < 0.05$, ** indicates $P < 0.01$, *** indicates $P < 0.001$, **** indicates $P < 0.0001$. Sample sizes and used analyses are listed in the corresponding figure legends. All western blots and cell death assays shown are representative of at least three independent experiments conducted in the laboratory.

Data availability

This study includes no data deposited in external repositories.

Expanded View for this article is available [online](#).

Acknowledgements

We thank M. Menning, A. Manav and T. Roth for their technical assistance. This work was supported by the German Cancer Aid (70114685 and 70114225), SFB1403 (project number 414786233), SFB1530 (project number 455784452) and SFB1218 (project number 269925409). We thank the CECAD animal facility (University of Cologne, Germany) for support with the animal work included in this study. Open Access funding enabled and organized by Projekt DEAL.

Author contributions

Fabian Schorn: Conceptualization; data curation; formal analysis; validation; investigation; visualization; methodology; writing – original draft. **J Paul Werthenbach:** Data curation; investigation; visualization; methodology; writing – original draft; writing – review and editing. **Mattes Hoffmann:** Formal analysis; investigation; methodology. **Mila Daoud:** Data curation; formal analysis; investigation; visualization; methodology. **Johanna Stachelscheid:** Formal analysis; investigation; visualization; methodology; writing – review and editing. **Lars M Schiffmann:** Investigation; methodology; writing – original draft; writing – review and editing. **Ximena Hildebrandt:** Investigation. **Su Ir Lyu:** Investigation. **Nieves Peltzer:** Resources. **Alexander Quaas:** Formal analysis; methodology. **Domagoj Vucic:** Resources. **John Silke:** Resources; writing – review and editing. **Manolis Pasparakis:** Resources. **Hamid Kashkar:** Conceptualization; resources; supervision; funding acquisition; methodology; writing – original draft; project administration; writing – review and editing.

Disclosure and competing interests statement

The authors declare that they have no conflict of interest.

References

- Anderton H, Bandala-Sanchez E, Simpson DS, Rickard JA, Ng AP, Di Rago L, Hall C, Vince JE, Silke J, Liccardi G *et al* (2019) RIPK1 prevents TRADD-driven, but TNFR1 independent, apoptosis during development. *Cell Death Differ* 26: 877–889
- Andree M, Seeger JM, Schull S, Coutelle O, Wagner-Stippich D, Wiegmann K, Wunderlich CM, Brinkmann K, Broxtermann P, Witt A *et al* (2014) BID-dependent release of mitochondrial SMAC dampens XIAP-mediated immunity against Shigella. *EMBO J* 33: 2171–2187
- Annibaldi A, Wicky John S, Vanden Berghe T, Swatek KN, Ruan J, Liccardi G, Bianchi K, Elliott PR, Choi SM, Van Coillie S *et al* (2018) Ubiquitin-mediated regulation of RIPK1 kinase activity independent of IKK and MK2. *Mol Cell* 69: 566–580.e5
- Bertrand MJ, Milutinovic S, Dickson KM, Ho WC, Boudreault A, Durkin J, Gillard JW, Jaquith JB, Morris SJ, Barker PA (2008) cIAP1 and cIAP2 facilitate cancer cell survival by functioning as E3 ligases that promote RIP1 ubiquitination. *Mol Cell* 30: 689–700
- Brightbill HD, Suto E, Blaquiére N, Ramamoorthi N, Sujatha-Bhaskar S, Gogol EB, Castaneda GM, Jackson BT, Kwon YC, Haller S *et al* (2018) NF-kappaB inducing kinase is a therapeutic target for systemic lupus erythematosus. *Nat Commun* 9: 179
- Conte D, Holcik M, Lefebvre CA, Lacasse E, Picketts DJ, Wright KE, Korneluk RG (2006) Inhibitor of apoptosis protein cIAP2 is essential for lipopolysaccharide-induced macrophage survival. *Mol Cell Biol* 26: 699–708
- Conze DB, Albert L, Ferrick DA, Goeddel DV, Yeh WC, Mak T, Ashwell JD (2005) Posttranscriptional downregulation of c-IAP2 by the ubiquitin protein ligase c-IAP1 *in vivo*. *Mol Cell Biol* 25: 3348–3356
- Conze DB, Zhao Y, Ashwell JD (2010) Non-canonical NF-kappaB activation and abnormal B cell accumulation in mice expressing ubiquitin protein ligase-inactive c-IAP2. *PLoS Biol* 8: e1000518
- Daoud M, Broxtermann PN, Schorn F, Werthenbach JP, Seeger JM, Schiffmann LM, Brinkmann K, Vucic D, Tuting T, Mauch C *et al* (2022) XIAP promotes melanoma growth by inducing tumour neutrophil infiltration. *EMBO Rep* 23: e53608
- Dowling JP, Alsabbagh M, Del Casale C, Liu ZG, Zhang J (2019) TRADD regulates perinatal development and adulthood survival in mice lacking RIPK1 and RIPK3. *Nat Commun* 10: 705

- Dumetier B, Zadoroznyj A, Dubrez L (2020) IAP-mediated protein ubiquitination in regulating cell signaling. *Cell* 9: 1118
- Ermolaeva MA, Michallet MC, Papadopoulou N, Utermohlen O, Kranidioti K, Kollias G, Tschopp J, Pasparakis M (2008) Function of TRADD in tumor necrosis factor receptor 1 signaling and in TRIF-dependent inflammatory responses. *Nat Immunol* 9: 1037–1046
- Emetadi N, Chopin M, Anderton H, Tanzer MC, Rickard JA, Abeyskera W, Hall C, Spall SK, Wang B, Xiong Y et al (2015) TRAF2 regulates TNF and NF- κ B signalling to suppress apoptosis and skin inflammation independently of Sphingosine kinase 1. *Elife* 4: e10592
- Feltham R, Bettjeman B, Budhidarmo R, Mace PD, Shirley S, Condon SM, Chunduru SK, McKinlay MA, Vaux DL, Silke J et al (2011) Smac mimetics activate the E3 ligase activity of cIAP1 protein by promoting RING domain dimerization. *J Biol Chem* 286: 17015–17028
- Fritsch M, Gunther SD, Schwarzer R, Albert MC, Schorn F, Werthenbach JP, Schiffmann LM, Stair N, Stocks H, Seeger JM et al (2019) Caspase-8 is the molecular switch for apoptosis, necroptosis and pyroptosis. *Nature* 575: 683–687
- Giardino Torchia ML, Conze DB, Ashwell JD (2013) c-IAP1 and c-IAP2 redundancy differs between T and B cells. *PLoS One* 8: e66161
- Haas TL, Emmerich CH, Gerlach B, Schmukle AC, Cordier SM, Rieser E, Feltham R, Vince J, Warnken U, Wenger T et al (2009) Recruitment of the linear ubiquitin chain assembly complex stabilizes the TNF-R1 signaling complex and is required for TNF-mediated gene induction. *Mol Cell* 36: 831–844
- Hsu H, Xiong J, Goeddel DV (1995) The TNF receptor 1-associated protein TRADD signals cell death and NF- κ B activation. *Cell* 81: 495–504
- Hsu H, Shu HB, Pan MG, Goeddel DV (1996) TRADD-TRAF2 and TRADD-FADD interactions define two distinct TNF receptor 1 signal transduction pathways. *Cell* 84: 299–308
- Kashkar H (2010) X-linked inhibitor of apoptosis: a chemoresistance factor or a hollow promise. *Clin Cancer Res* 16: 4496–4502
- Kearney CJ, Cullen SP, Clancy D, Martin SJ (2014) RIPK1 can function as an inhibitor rather than an initiator of RIPK3-dependent necroptosis. *FEBS J* 281: 4921–4934
- Kist M, Komuves LG, Goncharov T, Dugger DL, Yu C, Roose-Girma M, Newton K, Webster JD, Vucic D (2021) Impaired RIPK1 ubiquitination sensitizes mice to TNF toxicity and inflammatory cell death. *Cell Death Differ* 28: 985–1000
- Liston P, Roy N, Tamai K, Lefebvre C, Baird S, Cherton-Horvat G, Farahani R, McLean M, Ikeda JE, MacKenzie A et al (1996) Suppression of apoptosis in mammalian cells by NAIP and a related family of IAP genes. *Nature* 379: 349–353
- Mace PD, Linke K, Feltham R, Schumacher FR, Smith CA, Vaux DL, Silke J, Day CL (2008) Structures of the cIAP2 RING domain reveal conformational changes associated with ubiquitin-conjugating enzyme (E2) recruitment. *J Biol Chem* 283: 31633–31640
- Mahoney DJ, Cheung HH, Mrad RL, Plenchette S, Simard C, Enwere E, Arora V, Mak TW, Lacasse EC, Waring J et al (2008) Both cIAP1 and cIAP2 regulate TNF α -mediated NF- κ B activation. *Proc Natl Acad Sci USA* 105: 11778–11783
- Micheau O, Tschopp J (2003) Induction of TNF receptor I-mediated apoptosis via two sequential signaling complexes. *Cell* 114: 181–190
- Morrish E, Brumatti G, Silke J (2020) Future therapeutic directions for Smac-Mimetics. *Cell* 9: 406
- Moujalled DM, Cook WD, Okamoto T, Murphy J, Lawlor KE, Vince JE, Vaux DL (2013) TNF can activate RIPK3 and cause programmed necrosis in the absence of RIPK1. *Cell Death Dis* 4: e465
- Moulin M, Anderton H, Voss AK, Thomas T, Wong WW, Bankovacki A, Feltham R, Chau D, Cook WD, Silke J et al (2012) IAPs limit activation of RIP kinases by TNF receptor 1 during development. *EMBO J* 31: 1679–1691
- Newton K (2020) Multitasking kinase RIPK1 regulates cell death and inflammation. *Cold Spring Harb Perspect Biol* 12: a036368
- Newton K, Dugger DL, Maltzman A, Greve JM, Hedehus M, Martin-McNulty B, Carano RA, Cao TC, van Bruggen N, Bernstein L et al (2016) RIPK3 deficiency or catalytically inactive RIPK1 provides greater benefit than MLKL deficiency in mouse models of inflammation and tissue injury. *Cell Death Differ* 23: 1565–1576
- Park SM, Yoon JB, Lee TH (2004) Receptor interacting protein is ubiquitinated by cellular inhibitor of apoptosis proteins (c-IAP1 and c-IAP2) *in vitro*. *FEBS Lett* 566: 151–156
- Polykratis A, Hermance N, Zelic M, Roderick J, Kim C, Van TM, Lee TH, Chan FKM, Pasparakis M, Kelliher MA (2014) Cutting edge: RIPK1 Kinase inactive mice are viable and protected from TNF-induced necroptosis *in vivo*. *J Immunol* 193: 1539–1543
- Ramakers C, Ruijter JM, Deprez RH, Moorman AF (2003) Assumption-free analysis of quantitative real-time polymerase chain reaction (PCR) data. *Neurosci Lett* 339: 62–66
- Rothe M, Pan MG, Henzel WJ, Ayres TM, Goeddel DV (1995) The TNFR2-TRAF signaling complex contains two novel proteins related to baculoviral inhibitor of apoptosis proteins. *Cell* 83: 1243–1252
- Samuel T, Welsh K, Lober T, Togo SH, Zapata JM, Reed JC (2006) Distinct BIR domains of cIAP1 mediate binding to and ubiquitination of tumor necrosis factor receptor-associated factor 2 and second mitochondrial activator of caspases. *J Biol Chem* 281: 1080–1090
- Schiffmann LM, Werthenbach JP, Heintges-Kleinhofer F, Seeger JM, Fritsch M, Gunther SD, Willenborg S, Brodesser S, Lucas C, Jungst C et al (2020) Mitochondrial respiration controls neoangiogenesis during wound healing and tumour growth. *Nat Commun* 11: 3653
- Shu HB, Takeuchi M, Goeddel DV (1996) The tumor necrosis factor receptor 2 signal transducers TRAF2 and c-IAP1 are components of the tumor necrosis factor receptor 1 signaling complex. *Proc Natl Acad Sci USA* 93: 13973–13978
- Silke J (2011) The regulation of TNF signalling: what a tangled web we weave. *Curr Opin Immunol* 23: 620–626
- Silke J, Vaux DL (2015) IAP gene deletion and conditional knockout models. *Semin Cell Dev Biol* 39: 97–105
- Tang Y, Tu H, Zhang J, Zhao X, Wang Y, Qin J, Lin X (2019) K63-linked ubiquitination regulates RIPK1 kinase activity to prevent cell death during embryogenesis and inflammation. *Nat Commun* 10: 4157
- Uren AG, Pakusch M, Hawkins CJ, Puls KL, Vaux DL (1996) Cloning and expression of apoptosis inhibitory protein homologs that function to inhibit apoptosis and/or bind tumor necrosis factor receptor-associated factors. *Proc Natl Acad Sci USA* 93: 4974–4978
- Van Hauwermeiren F, Armaka M, Karagianni N, Kranidioti K, Vandenbroucke RE, Loges S, Van Roy M, Staelens J, Puimege L, Palagani A et al (2013) Safe TNF-based antitumor therapy following p55TNFR reduction in intestinal epithelium. *J Clin Invest* 123: 2590–2603
- Vanlangenakker N, Bertrand MJ, Bogaert P, Vandenabeele P, Vanden Berghe T (2011) TNF-induced necroptosis in L929 cells is tightly regulated by multiple TNFR1 complex I and II members. *Cell Death Dis* 2: e230
- Varfolomeev E, Vucic D (2022) RIP1 post-translational modifications. *Biochem J* 479: 929–951
- Varfolomeev E, Wayson SM, Dixit VM, Fairbrother WJ, Vucic D (2006) The inhibitor of apoptosis protein fusion c-IAP2.MALT1 stimulates NF- κ B activation independently of TRAF1 AND TRAF2. *J Biol Chem* 281: 29022–29029

- Varfolomeev E, Blankenship JW, Wayson SM, Fedorova AV, Kayagaki N, Garg P, Zobel K, Dynek JN, Elliott LO, Wallweber HJ *et al* (2007) IAP antagonists induce autoubiquitination of c-IAPs, NF-kappaB activation, and TNFalpha-dependent apoptosis. *Cell* 131: 669–681
- Varfolomeev E, Goncharov T, Fedorova AV, Dynek JN, Zobel K, Deshayes K, Fairbrother WJ, Vucic D (2008) c-IAP1 and c-IAP2 are critical mediators of tumor necrosis factor alpha (TNFalpha)-induced NF-kappaB activation. *J Biol Chem* 283: 24295–24299
- Vaux DL, Silke J (2005) IAPs, RINGs and ubiquitylation. *Nat Rev Mol Cell Biol* 6: 287–297
- Vince JE, Wong WW, Khan N, Feltham R, Chau D, Ahmed AU, Benetatos CA, Chunduru SK, Condon SM, McKinlay M *et al* (2007) IAP antagonists target cIAP1 to induce TNFalpha-dependent apoptosis. *Cell* 131: 682–693
- Vince JE, Pantaki D, Feltham R, Mace PD, Cordier SM, Schmukle AC, Davidson AJ, Callus BA, Wong WW, Gentle IE *et al* (2009) TRAF2 must bind to cellular inhibitors of apoptosis for tumor necrosis factor (tnf) to efficiently activate nf-kappaB and to prevent tnf-induced apoptosis. *J Biol Chem* 284: 35906–35915
- Wong WW, Gentle IE, Nachbur U, Anderton H, Vaux DL, Silke J (2010) RIPK1 is not essential for TNFR1-induced activation of NF-kappaB. *Cell Death Differ* 17: 482–487
- Yeh WC, Shahinian A, Speiser D, Kraunus J, Billia F, Wakeham A, de la Pompa JL, Ferrick D, Hum B, Iscove N *et al* (1997) Early lethality, functional NF-kappaB activation, and increased sensitivity to TNF-induced cell death in TRAF2-deficient mice. *Immunity* 7: 715–725
- Zarnegar BJ, Wang Y, Mahoney DJ, Dempsey PW, Cheung HH, He J, Shiba T, Yang X, Yeh WC, Mak TW *et al* (2008) Noncanonical NF-kappaB activation requires coordinated assembly of a regulatory complex of the adaptors cIAP1, cIAP2, TRAF2 and TRAF3 and the kinase NIK. *Nat Immunol* 9: 1371–1378
- Zhang J, Webster JD, Dugger DL, Goncharov T, Roose-Girma M, Hung J, Kwon YC, Vucic D, Newton K, Dixit VM (2019a) Ubiquitin ligases cIAP1 and cIAP2 limit cell death to prevent inflammation. *Cell Rep* 27: 2679–2689.e3
- Zhang X, Zhang H, Xu C, Li X, Li M, Wu X, Pu W, Zhou B, Wang H, Li D *et al* (2019b) Ubiquitination of RIPK1 suppresses programmed cell death by regulating RIPK1 kinase activation during embryogenesis. *Nat Commun* 10: 4158



License: This is an open access article under the terms of the [Creative Commons Attribution-NonCommercial-NoDerivs](https://creativecommons.org/licenses/by-nc-nd/4.0/) License, which permits use and distribution in any medium, provided the original work is properly cited, the use is non-commercial and no modifications or adaptations are made.